Chemical Engineering Journal 95 (2003) 179–186

Chemical Engineering Journal

www.elsevier.com/locate/cej

Effects of nano-Ag particles loading on TiO_2 photocatalytic reduction of selenate ions

T.T.Y. Tan, C.K. Yip, D. Beydoun, R. Amal*

Centre for Particle and Catalyst Technologies, School of Chemical Engineering and Industrial Chemistry, University of New South Wales, Sydney, NSW 2052, Australia

Abstract

The photocatalytic reduction of selenate Se(VI) ions was studied using unmodified TiO_2 and Ag-loaded TiO_2 (Ag-TiO_2) photocatalysts. In the presence of formic acid, both the TiO_2 and Ag-TiO_2 photocatalysts were effective in reducing Se(VI). The reaction proceeded through the reduction of Se(VI) ions to elemental selenium Se and then to hydrogen selenide gas (H_2Se). When unmodified TiO_2 photocatalyst was used, the Se formed from the reduction of Se(VI) was further reduced to Se^{2-} in the form of H_2Se upon the exhaustion of Se(VI) in solution. In the presence of the Ag-TiO_2 photocatalysts, hydrogen selenide gas was generated simultaneously with the reduction of Se(VI). It was found that the maximum Se(VI) reduction rate occurred at pH 3.5 and at a 0.5 at.% Ag loading while the maximum hydrogen selenide gas generation occurred at pH 3.5 and at 2.0 at.% Ag loading. The simultaneous reduction of Se(VI) to hydrogen selenide gas can be attributed to efficient charge separation due to the mediation of photogenerated electrons by the Ag particles. A mechanism is proposed in terms of the TiO_2-Ag-Se electronic interaction during UV irradiation.

Keywords: Nano-Ag; Photocatalysis; Reduction; Titanium dioxide; Selenate

1. Introduction

Photocatalysis has emerged to be one of the most promising pollution remediation technologies in recent decades. This technology can make use of the energy from the sun, which advocates energy sustainability. Semiconductor photocatalysts generate electron and hole pairs upon irradiation by light energy above a threshold which is characteristic of the semiconductor material. The holes and electrons could be utilised in initiating oxidation and reduction reactions, respectively [1,2]. Of all the photocatalysts, TiO_2 is the most widely studied one. It is very stable, cheap to produce and is capable of degrading a wide range of organic pollutants due to the positions of its valance and conduction bands [3].

Numerous studied have shown that photocatalytic technology is capable of degrading and mineralising a variety of harmful organic pollutants such as pesticides, insecticides and aromatic organics into innocuous products [4–6]. This technology has also been applied for heavy metal ions reduction, whereby the toxic heavy metal ions are reduced into their insoluble states for subsequent recovery or removal from industrial effluent [7,8]. One such example is the reduction of Ag^+ ions to Ag metal onto TiO_2 [9]. The Ag metal could then be recovered by digestion with nitric acid.

However, the semiconductor TiO_2 has its shortcomings. Due to its wide bandgap, it can only be activated by near-UV radiation. Near-UV radiation, on the other hand, constitutes about 4–5% of the natural sunlight. Also, the photogenerated electron–hole pairs tend to recombine easily, leading to very low quantum yields [10,11]. These problems have motivated scientists to find ways of increasing the TiO_2 photoresponse by shifting its adsorption to the visible light region and preventing the recombination of electron and holes.

For the former problem, ions have been doped into the lattice of the TiO_2 crystals [12]. This modifies the electronic structure of TiO_2 by narrowing the bandgap, rendering the doped TiO_2 more sensitive to the visible light. Attempts have also been made to sensitise the TiO_2 by loading the catalyst with dyes [13] and in other cases with a semiconductor having a narrower bandgap so that it could be activated by visible light [14]. To tackle the electron–hole recombination problem, the TiO_2 surface has been modified by metal deposits such as Pt, Ag or Au [15–18]. This serves the purpose of mediating the electrons away from the TiO_2 surface, hence preventing them from recombining with the holes. This is due to the fact that when a metal of a work function is greater than that of the semiconductor with which it is in contact, a Schottky barrier is created which facilitates the

* Corresponding author. Tel.: +61-2-9385-4361; fax: +61-2-9385-5966.
E-mail address: r.amal@unsw.edu.au (R. Amal).

1385-8947/$ – see front matter © 2003 Elsevier Science B.V. All rights reserved.
doi:10.1016/S1385-8947(03)00103-7

transfer of electrons from the semiconductor to the metal [19]. Another way of improving the catalytic efficiency is to improve the adsorption of the reactants on the TiO_2 surface where. This can be achieved by metal deposits on the photocatalyst surface [20] as well as surface modifications with organics [21].

Selenium compounds can be toxic if ingested in large quantity [22]. The current permissible Se level in drinking water is 10 ppb [23]. Of all the selenium compounds, selenate (SeO_4^{2-}) poses the greatest threat as it is not easily adsorbed onto particulates. This means it is highly mobile and could easily end up in drinking water [24,25]. The removal of selenate by a cost-effective method is hence necessary. Photocatalysis could be a good method for selenate removal as it reduces the selenate ions into the immobilised form of elemental selenium, hence removing it from the effluent. The reduction of selenate follows the following equations [26,27]:

$$SeO_4^{2-} + 8H^+ + 6e^- \rightarrow Se^0 + 4H_2O, \quad E^0 = 0.9\,V \quad (1)$$

where E^0 is the standard reduction potential. Elemental selenium could be further reduced to H_2Se, a toxic gas [26–28]:

$$Se^0 + 2H^+ + 2e^- \rightarrow H_2Se, \quad E^0 = -0.3\,V \quad (2)$$

Photocatalytic reduction of Se(VI) could also serve to recover the elemental selenium which finds abundant use in the manufacturing industries. For example, Se is used in xerography [29] and more recently in X-ray image detectors [30] since, being a semiconductor itself, Se is an excellent photoconductor [31,32]. It also imparts a pink colour in glass and is added in steel to make it anti-corrosive [33].

Previous investigations have seen the successful photoreduction of Se(VI) to Se onto TiO_2 in the presence of formic acid and nitrogen gas [26,34,35]. Since many studies have observed enhanced reduction rates with metal-modified TiO_2 [36,37], the current investigation aims to elucidate the effect of Ag-modified TiO_2 on the photocatalytic reduction of selenate ions.

2. Experimental section

2.1. Photoreactor and light source

A cylindrical glass photoreactor of 1.2 l capacity was used in the experiments. It consists of a side quartz-window where UV was illuminated through by a 200 W Mercury lamp (Oriel 66001-373). This lamp mainly provided light of wavelength below 380 nm, peaking at 254, 295, 315 and 370 nm. The reactor was placed on top of a magnetic stirrer for agitation, while the purging of nitrogen gas introduced from the top of the reactor served to agitate the contents and to provide an anoxic environment. Gas exhausted from the reactor was scrubbed by a copper(II) sulphate solution followed by a sodium hydroxide solution to ensure the removal of hydrogen selenide gas generated from the photoreduction experiments. The photon flux into the reactor was determined to be 3.8 μmol photon/s by chemical actinometry [38–40].

2.2. Preparation of Ag-TiO_2

The Ag-TiO_2 particles were prepared by photoreducing Ag^+ ions (from $AgNO_3$, 99.99 wt.%, Aldrich) to Ag metal on the TiO_2 surface. The TiO_2 used was Degussa P25. Four grams of TiO_2 were added into 1 l of ultra-pure water in the photoreactor and then irradiated for 10 min to remove any impurities that might be present on the TiO_2 surface. Aliquots of various amounts of Ag^+ ions, prepared by dissolving silver nitrate salt in deionised water, were added into the suspension of TiO_2 such that the Ag^+ concentration was of 0.5, 1.0, 2.0 and 5.0 at.% in relation to TiO_2. In this paper, the various Ag/TiO_2 samples prepared are identified by the Ag^+ loading (at.%) added to the suspension prior to the illumination of the suspension. Sucrose (supplied by Fisons Scientific Equipment) was added to act as the hole scavenger. The suspension was adjusted to pH 3.5 by perchloric acid and then irradiated for 40 min with continuous nitrogen purging. The suspension was then filtered, washed, dried and hand-ground to obtain the Ag-deposited TiO_2 particles.

2.3. Experimental procedures for adsorption and Se(VI) photoreduction

The reaction suspensions were prepared by adding a pre-sonicated solution containing 0.5 g of Ag-TiO_2 catalyst into a solution consisting 0.254 mM Se(VI) (from sodium selenate) and 25 mMC formic acid to make up 1 l of suspension. The pH of the suspension was adjusted and controlled using perchloric acid and sodium hydroxide. Prior to UV irradiation, the suspension was stirred for 0.5 h to establish adsorption equilibrium conditions. The suspension was then irradiated with constant stirring and nitrogen purging for 2 h. At given time intervals, samples were taken from the suspension and immediately filtered through a 0.45 μm Millipore filter to remove the particles. The filtrate was analysed as required.

2.4. Electrophoresis experiments

Suspensions containing approximately 20 ppm particles (unmodified or Ag-modified TiO_2) and 0.1 mM NaCl were prepared. Dilute HCl and NaOH solutions were added to the above suspensions to adjust to the desired pH. The suspensions were then subjected to electrophoresis analysis.

2.5. Analytical method

The total Se concentration (Se(VI)) in the filtrate was determined by Varian Induced Coupled Plasma-Atomic Emission Spectroscopy (ICP-AES). The amount of H_2Se

generated was determined by analysing the amount of Cu(II) remaining in the trap using Varian ICP-AES. Formic acid concentration was determined by analysing the total organic carbon (TOC) in the solution using Shimadzu TOC-5000A analyser. Powder X-ray diffraction (Siemens D5000 Diffractometer) was used to study the crystalline nature of the deposited Ag particles. The morphology of the Se particles and the Ag-deposited TiO_2 particles was examined using Transmission Electron Microscope (TEM, Phillips CM200). The TEM was supported by an Energy Dispersive X-Ray Spectometer (EDAX) that enables elemental identification of particles through mapping. Electrophoresis analysis was done by the Brookhaven 3-in-1 system.

3. Results and discussions

3.1. Characterisations of the Ag deposits on TiO_2

The Ag-deposited TiO_2 particles were brownish in colour. X-ray diffraction analysis was carried out and the presence of Ag-metal on the TiO_2 surface was confirmed. Mapping by EDAX from TEM also showed the presence of Ag on TiO_2 particles. This can be seen in Fig. 1, where the specks of Ag deposits on Fig. 1b were found to correspond with the area in which the Ti element was mapped (Fig. 1a). The size of the Ag deposits was found to be non-uniform and estimated to be less than 10 nm in diameter.

3.2. Photocatalytic reduction of Se(VI) by bare TiO_2 and Ag-deposited TiO_2

The photocatalytic reduction of Se(VI) was only observed in the presence of both formic acid and UV-irradiation. The colour of the suspension changed from white (TiO_2) or brown (Ag-TiO_2) to orange, indicating the photoreduction of Se(VI) to elemental Se onto the surface of the TiO_2. The presence of elemental Se was confirmed by TEM mapping (Fig. 1c). The Se particles formed on TiO_2 were round in shape (Fig. 1d). This corresponds to the position of the mapped Se elements as shown in Fig. 1c. Fig. 1d shows an image indicated by the boxed area in Fig. 1a. The position marked X on Fig. 1a shows an absence of the Ti signal from the mapping. This is due to the Se formed on top of the TiO_2 as shown in Fig. 1c and d. From Fig. 1d, it can also be seen that the Se particles formed are round and bigger relative to TiO_2. The following argument is put forward to explain the formation of the spherical Se particles. Our postulation is that the Se particles are acting as the reducing sites for Se(VI) ions, resulting in the growing of the Se particles. For this to be valid, the Se particles would have to be rich in electrons. With Se being a photoconductor and a

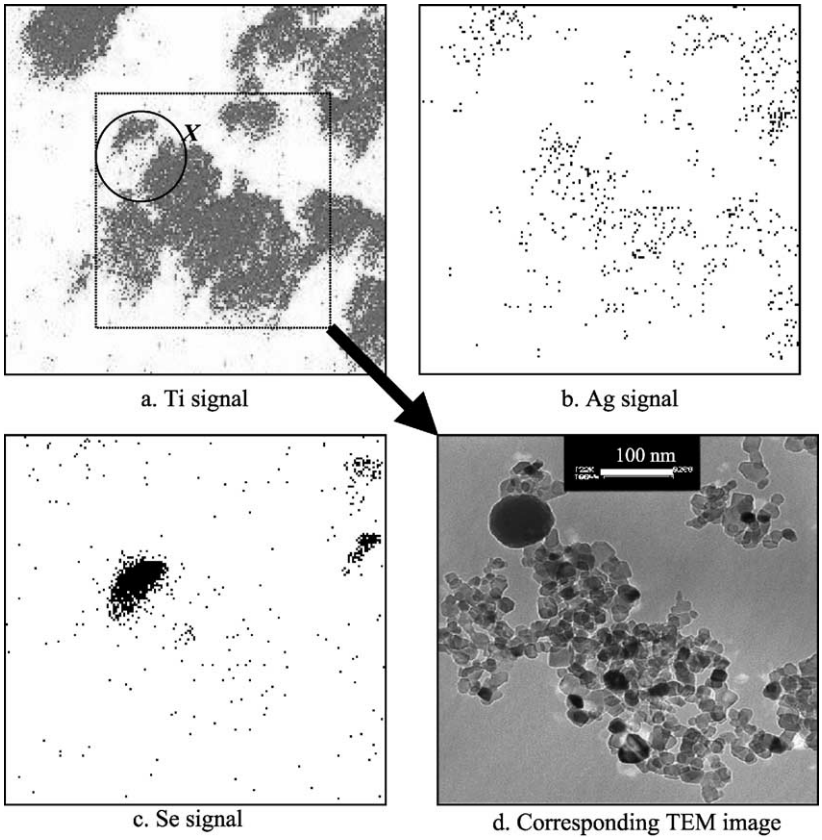

Fig. 1. Parts a, b and c show the mapping of Ti, Ag and Se, respectively, by TEM. Part d shows the corresponding TEM image of Se on TiO_2.

p-type semiconductor [41], it is possible for the photogenerated electrons in TiO_2 to be transferred to the Se particles making them rich in electrons, and hence making them the reducing sites for Se(VI) ions. A detailed mechanism of this electron-transfer mechanism is described elsewhere [42].

When unmodified TiO_2 was used, H_2Se generation was observed when the Se(VI) ions had been completely exhausted from the solution. The generation of H_2Se was indicated by the formation of black precipitates of CuSe in the Cu^{2+} scrubber. When Ag-TiO_2 was used as the photocatalyst, different observations were made. While Se(VI) was also photoreduced to elemental Se by Ag-TiO_2 in the presence of formic acid, H_2Se gas was simultaneously generated. Fig. 2a and b show the photoreduction of Se(VI) with the corresponding H_2Se generation for unmodified TiO_2 and Ag-TiO_2. From Fig. 2a, it could be seen that the complete removal of Se(VI) took about 270 min. This removal was due to the combined effect of adsorption and reduction. The decrease in Se(VI) concentration at time = 0 min indicated Se(VI) removal due to dark adsorption before the onset of UV irradiation. It has been shown that only the adsorbed Se(VI) ions could be reduced [35]. Upon irradiation, as the adsorbed Se(VI) ions on the TiO_2 surface were reduced to elemental Se and as the reaction proceeded, the concentration of Se(VI) in the solution decreased, indicating that the decrease of Se(VI) from the solution was primarily due to its reduction on the TiO_2 surface.

Fig. 2a showed that the onset of H_2Se generation occurred when the Se(VI) was nearly exhausted from the suspension. It also showed that formic acid was continuously oxidised as the reduction continued, an indication that the photogenerated holes were continuously utilised for the oxidation of the formic acid. The following postulation is put forward to explain these observations. It was believed that the electrons were continuously being transferred from the TiO_2 to the Se particles even after Se(VI) ions were exhausted from the suspension. This caused the accumulation of electrons in the Se particles, enabling the self-reduction of Se to H_2Se since the reduction potential of Se/Se^{2-} lies within the bandgap of the Se semiconductor (as indicated in Fig. 3). Kikuchi and Sakamoto have shown the accumulation of electrons in the suspension towards the end of the Se(VI) reduction

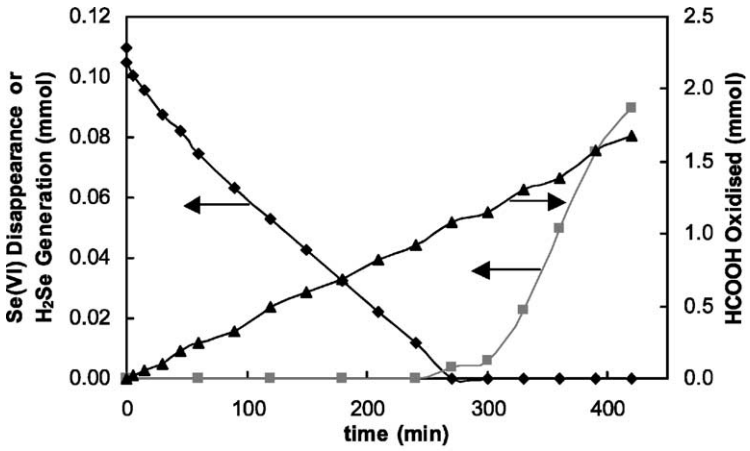

(a) Unmodified TiO_2

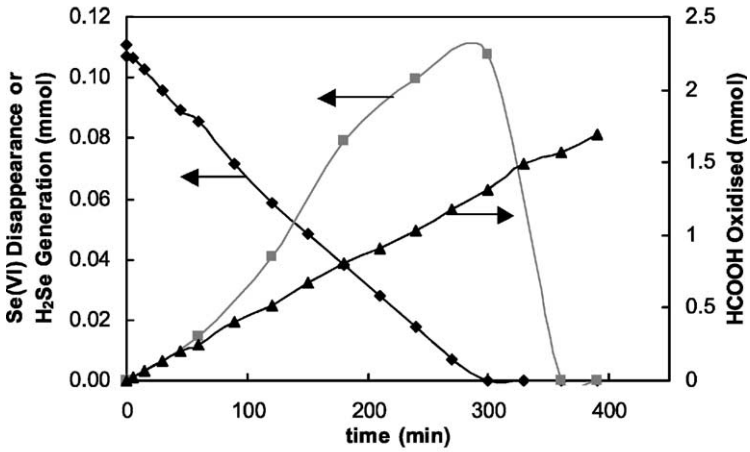

(b) 2 atomic % Ag-TiO_2

Fig. 2. Se(VI) photoreduction experiments performed using unmodified TiO_2 and Ag-TiO_2. (◆) Se(VI) concentration, (■) H_2Se generation, (▲) formic acid oxidation.

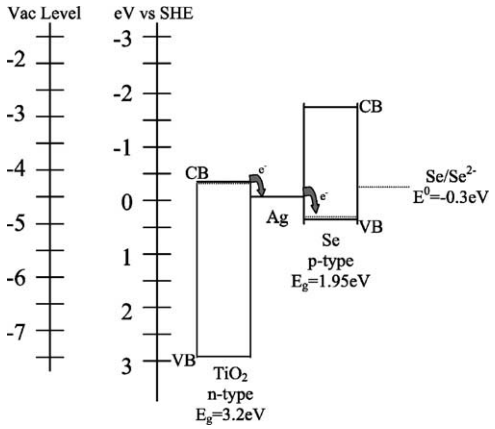

Fig. 3. Energy diagram of the TiO_2-Ag-Se system at pH 3.5. Bandgap energy (E_g): $E_{g\text{-}TiO_2} = 3.2$ eV [13,20], $E_{g\text{-}Se} = 1.95$ eV [41]. Conduction band potential (CB): $CB_{TiO_2} = -0.3$ eV [20,44], $CB_{Se} = -1.65$ eV [41]. Work function (Φ): $\Phi_{TiO_2} = 4.2$ eV, $\Phi_{Ag} = 4.6$ eV, $\Phi_{Se} = 4.8$ eV (assuming Fermi levels are near the conduction and valence band for TiO_2 and Se, respectively, and the work functions are calculated by the equations given in [45]).

reactions by measuring the potential of the suspension. They proposed an electron accumulation model in support of their findings [43].

As mentioned earlier, the Ag-TiO_2 photocatalyst behaved differently to the TiO_2 photocatalyst. The simultaneous generation of H_2Se and reduction of Se(VI) using the Ag-TiO_2 as a photocatalyst (as shown in Fig. 2b) may be explained as follows. When two materials of different work functions are in contact, an energy barrier for electron transfer is created at the junction. This is sometimes known as the Schottky barrier [19]. The transfer of electrons is facilitated from a material of lower work function to one that has a higher work function. For the TiO_2-Ag-Se system, the work function of Ag is greater than that of TiO_2 while that of Se is greater than that of Ag. Electrons can hence be transferred from TiO_2 to Ag and then to Se as the energy barrier for electron transfer from Ag to TiO_2 or from Se to Ag is higher than that of the opposite. Many studies involving surface modification of TiO_2 by metal loading such as Ag [20] and Au [18,46] have explained the transfer of electron with this theory. The above explanation is further illustrated in Fig. 3 where the relative bandgaps and work functions of these materials and the direction of electrons transfer are shown.

In the presence of Ag metal on TiO_2, it is postulated that the photogenerated electrons transferred from TiO_2 to Se via Ag result in the accumulation of electrons in the Se particles even before the exhaustion of Se(VI) in the solution, resulting in the reduction of Se to Se^{2-}. It is also important to note that the electrons transferred from the TiO_2 particles via the Ag metal would not have enough reducing power to initiate the reduction of Se to Se^{2-} as the conduction band of TiO_2 is lower than that of the reduction potential of Se/Se^{2-}. Otherwise, H_2Se would have been generated by the unmodified TiO_2 before the exhaustion of Se(VI) ions. When unmodified TiO_2 was used, it is postulated that the accumulation of electrons in the Se semiconductor becomes more significant only upon exhaustion of Se(VI) ions, enabling the further reduction of Se to H_2Se [42]. The presence of Ag on TiO_2 greatly increased the transfer of electrons from the TiO_2 to Se, making the self reduction of Se possible even before the exhaustion of Se(VI) ions.

When further analysing the photoreduction process using the Ag-TiO_2 photocatalyst, it was observed that the rate of Se(VI) reduction was slower compared to that when unmodified TiO_2 was used. This suggests that there was a

Table 1
Summary of results for Se(VI) photoreduction using unmodified and Ag-TiO_2 at various Ag loading and pH

Experiment no.	Ag (at.%) on TiO_2	H_2Se generated in 120 min ($\times 10^{-2}$ mmol, ±2% error)	Se(VI) reduced in 120 min ($\times 10^{-2}$ mmol, ±2% error)	Formic oxidised in 120 min ($\times 10^{-1}$ mmol, ±4% error)
pH = 2.5				
1.1	0.0	0.00	5.26	3.33
1.2	0.5	0.249	5.81	3.40
1.3	1.0	0.800	5.71	3.29
1.4	2.0	1.10	5.19	3.58
1.5	5.0	0.844	4.62	3.42
pH = 3.5				
2.1	0.0	0.00	5.61	3.93
2.2	0.5	1.17	6.30	3.81
2.3	1.0	2.44	5.95	4.08
2.4	2.0	4.09	5.38	4.26
2.5	5.0	1.17	4.92	3.97
pH = 5.0				
3.1	0.0	0.00	3.76	2.52
3.2	0.5	0.231	4.06	2.27
3.3	1.0	0.487	4.15	2.45
3.4	2.0	0.950	3.54	2.55
3.5	5.0	0.667	2.80	2.13

competition for the available electrons for both the reduction of Se(VI) to Se and of Se to H_2Se.

In order to further the understanding of the photoreduction mechanism using Ag-TiO_2, photocatalysts with different Ag loading were prepared. The pH of the system was also varied. The results are summarised in Table 1. The effect of Ag loading will be discussed first. From the results it can be seen that the simultaneous H_2Se generation was encountered in all cases when Ag-TiO_2 was used. When comparing the different at.% of Ag-deposited on TiO_2 particles, it was found that increasing the Ag deposited amount resulted in the increase production of H_2Se gas up to 2 at.% Ag. These results are explained as follows. From TEM mapping, increasing the Ag loading was found to increase the Ag amount distributed on theTiO_2 surface, and hence increasing the chance of Ag in contact with Se, resulting in more H_2Se production. Nevertheless, when the highest Ag loading of 5.0 at.% was used, both H_2Se generation and Se(VI) reduction seemed to be suppressed. An optimum metal loading has been previously reported with a number of explanations for its occurrence given [16,18]. These include the decrease in the available active sites and the competition for light absorption between the Ag and TiO_2 particles, hence resulting in a lower quantum efficiency.

Adsorption studies were carried out on the Ag-TiO_2 and unmodified TiO_2 in order to explain their different performance. Electrophoresis analysis was also carried out on unmodified, 0.5 at.% Ag and 5.0 at.% Ag-TiO_2. The results are presented in Fig. 4. The point of zero charge for unmodified Degussa TiO_2 particles was found to be at pH 5.6. The Ag-TiO_2 did not show significant difference in electrophoresis in comparison with unmodified TiO_2. It could hence be assumed that the adsorption of Se(VI) and formate ions by unmodified and modified TiO_2 is relatively similar.

The effect of pH on the Se(VI) photoreduction was also investigated. When the photocatalytic performance of the same Ag loading were compared at different pH values, for example, comparing experiment nos. 1.3, 2.3 and 3.3 in Table 1, it can be seen that the fastest rate of Se(VI) photoreduction occurred at pH 3.5 even though the adsorption of Se(VI) was greater at pH 2.5 than that at pH 3.5. Fig. 5 shows the dark adsorption of selenate and formate in the dark in the pH range of 2.5–5.0. It was found that the Se(VI) adsorption was significantly lowered while formate ions adsorption was increased when the pH was increased from 2.5 to 5.0. The decrease of Se(VI) adsorption could be attributed to the decrease in the surface positive charge as pH increased. However, the increase of formic adsorption was due to the improved ionisation of formic acid ($pK_a = 3.77$) [47] into formate ions as pH was raised. This increased the amount of negatively charged formate ions in the suspension and hence improved the equilibrium adsorption charged formate ions in the suspension and hence improved the equilibrium adsorption of the ions. The optimum pH at pH 3.5 could be explained by the increased formate ions adsorption which provided more hole scavengers for the reaction, hence increasing the availability of electrons for the reduction of Se(VI) ions [35]. The slowest rate for Se(VI) reduction was found at pH 5.0. This was due to the very little Se(VI) adsorption at this pH. It was also found that the maximum Se(VI) reduction rate was encountered at pH 3.5 and at 0.5 at.% Ag. This is an improvement of about 10% in terms

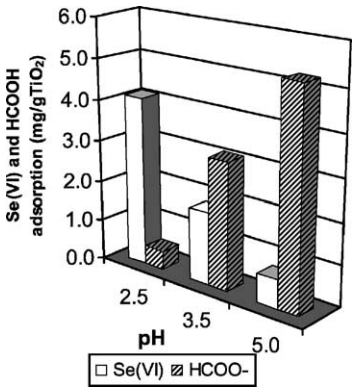

Fig. 5. Equilibrium dark adsorption of Se(VI) and HCOO ions on bare TiO_2 at various pH.

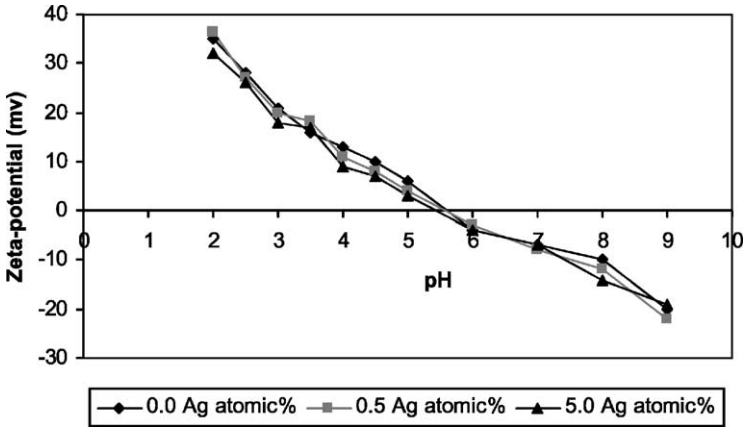

Fig. 4. Surface charge of TiO_2 and Ag-TiO_2 particles at various pH.

of the total Se(VI) reduced over a duration of 120 min when compared to unmodified TiO_2. However, at this optimum Ag-loading, H_2Se was simultaneously generated, which was an undesirable by-products due to its high toxicity. The highest amount of H_2Se generation was also encountered at pH 3.5 and was lowest at pH 5.0. It could hence be said that the rate of H_2Se generation was dependent on the rate of Se(VI) reduced. The lower amount of H_2Se formed at pH 5.0 could also be due to the lack of H^+ ions in the suspension at that pH. According to Eq. (2), H^+ ions are necessary for the formation of H_2Se.

By referring to Table 1 again, it was also found that the oxidation rate of formic acid was the highest at pH 3.5 and lowest at pH 5.0. This was expected since improved oxidation is an indication of more effective hole scavenging and hence effective electron scavenging. It is, therefore, not surprising that the optimum conditions for formic acid oxidation corresponded with that of Se(VI) reduction. It has also been reported that formate ions could directly transfer electrons to the valance band holes yielding formate radicals ($HCOO^{\bullet}$) and possible $CO_2^{\bullet -}$ radicals [48]. The role of these radicals and their subsequent formation to CO_2 have not been thoroughly discussed at this stage since this work focuses mainly on the photoreduction of Se(VI) while formic acid was used to complete the redox reactions. The role of various organic hole scavenger in the photoreduction of Se anions have been elucidated in our work published elsewhere [49].

4. Conclusions

Both unmodified and Ag-modified TiO_2 particles were able to photoreduce Se(VI) to elemental Se. In the case in which unmodified TiO_2 was used, H_2Se generation occurred only when the Se(VI) ions in the suspension were exhausted. However, H_2Se was generated simultaneously during the reduction of Se(VI) when Ag-TiO_2 was used. This was explained in terms of electron mediation from TiO_2 to Se via the Ag metals, greatly enhancing the electron density in the Se particles and hence leading to the formation of H_2Se via the self-reduction of Se. Increasing the Ag-loading amount (up to 2 at.% Ag) on TiO_2 resulted in greater H_2Se generation, possibly due to the greater amount of Ag metal loaded on the surface and hence increasing the chance of Se contact with Ag metals. It was found that at 0.5 at.% Ag-TiO_2, Se(VI) reduction rate was improved by an average of 10% at the pH investigated. Both Se(VI) reduction and H_2Se generation rate were found to be highest at pH 3.5. Formic acid oxidation rate increased with an increase in the reduction rates.

Acknowledgements

The author T. Tan would like to acknowledge the Australian Institute of Nuclear Science and Engineering (AINSE) for financial support and The University of New South Wales and the Department of Education, Training and Youth Affairs (DETYA) for awarding the International Postgraduate Research Scholarship. Special thanks to the Electron Microscopy Unit of UNSW for their assistance when using the TEM.

References

[1] A. Mills, S. Le Hunte, An overview of semiconductor photocatalysis, J. Photochem. Photobiol. A 108 (1997) 1–35.
[2] D. Chen, M. Sivakumar, A.K. Ray, Heterogeneous photocatalysis in environmental remediation, Dev. Chem. Eng. Min. Proc. 8 (5–6) (2000) 505–550.
[3] M.I. Litter, Review: heterogeneous photocatalysis transition metals ions in photocatalytic systems, Appl. Catal. B 23 (1999) 89–114.
[4] H. Al-Ekabi, N. Serpone, Kinetic studies in heterogeneous photocatalysis. 1. Photocatalytic degradation of chlorinated phenols in aerated aqueous solutions over TiO_2 supported on a glass matrix, J. Phys. Chem. 92 (1988) 5726–5731.
[5] B. Pal, M. Sharon, Photodegradation of polyaromatic hydrocarbons over thin film of TiO_2 nanoparticles: a study of intermediate photoproducts, J. Mol. Catal. A 160 (2) (2000) 453–460.
[6] C.S. Turchi, D.F. Ollis, Mixed reactant photocatalysis: intermediates and mutual rate inhibition, J. Catal. 119 (1989) 483–496.
[7] D. Chen, A.K. Ray, Removal of toxic metal ions from wastewater by semiconductor photocatalysis, Chem. Eng. Sci. 56 (2001) 1561–1570.
[8] K. Tennakone, K.G.U. Wijayantha, Heavy-metal extraction from aqueous medium with an immobilized TiO_2 photocatalyst and a solid sacrificial agent, J. Photochem. Photobiol. A 113 (1998) 89–92.
[9] M. Huang, E. Tso, A.K. Datye, M.R. Prairie, B.M. Stange, Removal of silver in photographic processing waste by TiO_2-based photocatalysis, Environ. Sci. Tech. 30 (1996) 3084–3088.
[10] A. Kudo, M. Sekizawa, Photocatalytic H_2 evolution under visible light irradiation on Ni-doped ZnS photocatalyst, Chem. Commun. (2000) 1371–1373.
[11] K. Sayamana, H. Arakawa, Effect of carbonate salt addition on the photocatalytic decomposition of liquid water over Pt-TiO_2, J. Chem. Soc., Faraday Trans. 93 (8) (1997) 1647–1655.
[12] H. Yamashita, M. Harada, J. Misaka, M. Takeuchi, K. Ikeue, M. Anpo, Degradation of propanol diluted in water under visible light irradiation using metal ion-implanted titanium dioxide photocatalysts, J. Photochem. Photobiol. A 6003 (2002) 1–5.
[13] A. Hagfeldt, M. Gratzel, Light-induced redox reactions in nanocrystalline systems, Chem. Rev. 95 (1) (1995) 49–68.
[14] L. Spanbel, H. Weller, A. Henglein, Photochemistry of semiconductor colloids. 22. Electron injection from illuminated CdS into attached TiO_2 and ZnO particles, J. Am. Chem. Soc. 109 (1987) 6632–6635.
[15] J.C. Yang, Y.C. Kim, Y.G. Shul, C.H. Shin, T.K. Lee, Characterization of photoreduced Pt/TiO_2 and decomposition of dichloroacetic acid over photoreduced Pt/TiO_2 catalysts, Appl. Surf. Sci. 121/122 (1997) 525–529.
[16] V. Vamathevan, H. Tse, R. Amal, G. Low, S. McEvoy, Effects of Fe^{3+} and Ag^+ ions on the photocatalytic degradation of sucrose in water, Catal. Today 68 (2001) 201–208.
[17] C. Xi, Z. Chen, Q. Li, Z. Jin, Effects of H^+, Cl^- and CH_3COOH on the photocatalytic conversion of $PtCl_6^{2-}$ in aqueous TiO_2 dispersion, J. Photochem. Photobiol. A 87 (3) (1995) 249–255.
[18] X.Z. Li, F.B. Li, Study of Au/Au^{3+}-TiO_2 photocatalysts toward visible photooxidation for water and wastewater treatment, Environ. Sci. Tech. 35 (11) (2001) 2381–2387.
[19] R. Dalven, Physics of Metal–Semiconductor and Metal–Insulator–Semiconductor Junctions, Introduction to Applied Solid State Physics, 2nd ed., Plenum Press, New York, London, 1990, Chapter 4, pp. 111–128.

[20] H. Tada, K. Teranishi, Y. Inubushi, S. Ito, TiO_2 photocatalytic reduction of bis(2-dipyridyl)disulfide to 2-mercaptopyridine by H_2O: incorporation effect of nanometer-sized Ag particles, Chem. Commun. (1998) 2345–2346.
[21] C.R. Chenthamarakshan, K. Rajeshwar, Photocatalytic reduction of divalent zinc and cadmium ions in aqueous TiO_2 suspensions: an interfacial induced adsorption-reduction pathway mediated by formate ions, Electrochem. Commun. 22 (2000) 527–530.
[22] H.M. Ohlendorf, D.J. Hoffman, M.K. Saiki, T.W. Aidrich, Embryonic mortality and abnormalities of aquatic birds: apparent impacts of selenium from irrigation drainwater, Sci. Total Environ. 52 (1986) 49–63.
[23] M.J. Jones, R. French, Local Government Engineering in Australia, The Federation Press, 1999.
[24] P. Zhang, D.L. Sparks, Kinetics of selenate and selenite adsorption/desorption at the goethite/water interface, Environ. Sci. Tech. 24 (1990) 1848–1856.
[25] Y. Zhang, J.N. Moore, Interaction of selenate with a wetland sediment, Appl. Geochem. 12 (1997) 685–691.
[26] S. Sanuki, T. Kojima, K. Arai, S. Nagaoka, H. Majima, Photocatalytic reduction of selenate and selenite solutions using TiO_2 powders, Metall. Mater. Trans. B 30B (1999) 15–20.
[27] F. Seby, M. Potin-Gautier, E. Giffaut, G. Borge, O.F.X. Donard, A critical review of thermodynamics data for selenium species at 25 °C, Chem. Geol. 171 (2001) 173–191.
[28] P.B. Linkson, The stability of selenium in aqueous system, Trans. Ind. Chem. Eng. 70B (1992) 149–152.
[29] S.O. Kasap, M. Baxendale, C. Juhasz, Xerographic properties of a-Se:Te photoconductors, IEEE Trans. Ind. Appl. 27 (4) (1991) 620–626.
[30] S.O. Kasap, C. Haugen, M. Nesdoly, J.A. Rowlands, Properties of a-Se for use in flat panel X-ray image detectors, J. Non-Cryst. Solids 266–269 (2000) 1163–1167.
[31] N.I. Ibragimov, Z.M. Abutalibova, V.G. Agaev, Electrophotographic layers of trigonal Se in the binder obtained by reduction of SeO_2 by hydrazine, Thin Solid Films 359 (1999) 125–126.
[32] R. Dalven, Detectors and Generators of EM Radiation, Introduction to Applied Solid State Physics, 2nd ed., Plenum Press, New York, London, 1990, Chapter 7, pp. 177–216.
[33] J.E. Oldfield, SeRendipity, Chemtech. March (1995) 52–55.
[34] S. Sanuki, K. Shako, S. Nagaoka, H. Majima, Photocatalytic reduction of Se ions using suspended anatase powders, Mater. Trans. JIM 41 (7) (2000) 799–805.
[35] T.Y. Tan, D. Beydoun, R. Amal, Photocatalytic reduction of Se(VI) in aqueous solutions in UV/TiO_2 system: importance of stoichiometric ratio of reactants on TiO_2 surface, J. Mol. Catal. A: Chem., in press.
[36] T.F. Xie, D.J. Wang, L.J. Zhu, T.J. Li, Y.J. Xu, Application of surface photovoltage technique in photocatalysis studies on modified TiO_2 photocatalysts for photoreduction of CO_2, Mater. Chem. Phys. 70 (2001) 103–106.
[37] Y. Kohno, H. Hayashi, S. Takenaka, T. Tanaka, T. Funabiki, S. Yoshida, Photoenhanced reduction of carbon dioxide with hydrogen over Rh/TiO_2, J. Photochem. Photobiol. A 126 (1999) 117–123.
[38] C.A. Parker, A new sensitive chemical actinometer. I. Some trials with potassium ferrioxalate, Proc. R. Soc. 220 (1953) 104–116.
[39] C.A. Parker, A new sensitive chemical actinometer. II. Potassium ferrioxalate as a standard chemical actinometer, Proc. R. Soc. (1953) 518–536.
[40] N.J. Bruce, Actinometry, in: J.C. Scarano (Ed.), CRC Handbook of Organic Photochemistry, vol. 1, CRC Press, Florida, 1989, Chapter 9, pp. 241–259.
[41] E.A. Streltsov, S.K. Poznyak, N.P. Osipovich, Photoinduced and dark underpotential deposition of lead on selenium, J. Electroanal. Chem. 518 (2002) 103–114.
[42] T.Y. Tan, M. Zaw, D. Beydoun, R. Amal, The formation of nano-sized selenium–titanium dioxide composite semiconductors by photocatalysis, 4 (6) (2002) 541–552.
[43] E. Kikuchi, H. Sakamoto, Kinetics of the reduction reaction of selenate ions by TiO_2 photocatalyst, J. Electrochem. Soc. 147 (12) (2000) 4589–4593.
[44] C.R. Chenthamarakshan, Y. Ming, K. Rajasehwar, Underpotential photocatalytic deposition: a new preparative route to composite semiconductors, Chem. Mater. 12 (2000) 3538–3540.
[45] A. Henglein, Nanoclusters of semiconductor and metals: colloidal nano-particles of semiconductors and metals: electronic structure and processes, Ber. Bunsenges. Phys. Chem. 11 (1997) 1562–1572.
[46] H. Tada, F. Suzuki, S. Yoneda, S. Ito, H. Kobayashi, The effect of nanometre-sized Au particle loading on TiO_2 photocatalysed reduction of bis(2-dipyridyl)disulfide to 2-mercaptopyridine by H_2O, Phys. Chem. Chem. Phys. 3 (7) (2001) 1376–1382.
[47] R. Chang, Acid–base equilibria, in: R. Chang (Ed.), Chemistry, 5th ed., McGraw-Hill, New York, 1994, Chapter 16, pp. 631–678.
[48] L.L. Perissinotti, M.A. Brusa, M.A. Grela, Yield of carboxyl anion radicals in the photocatalytic degradation of formate over TiO_2 particles, Langmuir 17 (2001) 8422–8427.
[49] T.Y. Tan, M. Zaw, D. Beydoun, R. Amal, Effects of organic hole scavengers on the photocatalytic reduction of Se ions, J. Photochem. Photobiol. A: Chem., in press.